Wydawnictwo UR 2020
ISSN 2544-1361 (online); ISSN 2544-2406
doi: 10.15584/ejcem.2020.1.5

http://www.ejcem.ur.edu.pl/en/
European Journal of Clinical and Experimental Medicine
Eur J Clin Exp Med 2020; 18 (1): 24–27

REVIEW PAPER

Adrian Truszkiewicz [1(ABDGF)], David Aebisher [1(ABDGF)], Zuzanna Bober [1(DG)], Łukasz Ożóg [1(DG)], Dorota Bartusik-Aebisher [2(ABDGF)]

Radio Frequency MRI coils

[1] Department of Photomedicine and Physical Chemistry, Medical College of Rzeszów University, Rzeszów, Poland
[2] Department of Biochemistry and General Chemistry, Medical College of Rzeszów University, Rzeszów, Poland

ABSTRACT

Introduction. Magnetic Resonance Imaging (MRI) coils technology is a powerful improvement for clinical diagnostics. This includes opportunities for mathematical and physical research into coil design.

Aim. Here we present the method applied to MRI coil array designs.

Material and methods. Analysis of literature and self-research**.**

Results. The coils that emit the radiofrequency pulses are designed similarly. As much as possible, they deliver the same strength of radiofrequency to all voxels within their imaging volume. Surface coils on the other hand are usually not embedded in cylindrical surfaces relatively close to the surface of the body.

Conclusion. The presented here results relates to the art of magnetic resonance imaging (MRI) and RF coils design. It finds particular application of RF coils in conjunction with bore type MRI scanners.

Keywords. field strength 1.5 Tesla, magnetic resonance imaging, radio frequency coil

Introduction

Radio Frequency (RF) coil is commonly used in configurations for MR imaging.[1-9] The RF signal emitted by tissue is detected by monitoring the alternating voltage induced in antenna wires near the patients.[10] These coils may be used also as to transmit the radio frequency pulses that are applied to the patient, or that separate coils may transmit the radio frequency emitted by the tissue may be detected using receive only coils.[12] The theoretical basis for the electromagnetic analysis is the solution of Maxwell equation for the electric field expressed in the terms of the vector and scalar potentials.[10-15]

$$\nabla \times \vec{E} = -\frac{\partial \vec{B}}{\partial t}$$

$$\nabla \times \vec{B} = \mu \vec{j} + \mu\varepsilon \frac{\partial \vec{E}}{\partial t} \qquad \text{(Equ. 1).}$$

$$\varepsilon \nabla \cdot \vec{E} = \rho$$

$$\nabla \cdot \vec{B} = 0$$

Corresponding author: Dorota Bartusik-Aebisher, e-mail: dbartusik-aebisher@ur.edu.pl

Participation of co-authors: A – Author of the concept and objectives of paper; B – collection of data; C – implementation of research; D – elaborate, analysis and interpretation of data; E – statistical analysis; F – preparation of a manuscript; G – working out the literature; H – obtaining funds

Received: 12.10.2019 | Accepted: 4.01.2020
Publication date: March 2020

Truszkiewicz A, Aebisher D, Bober Z, Ożóg Ł, Bartusik-Aebisher D. *Radio Frequency MRI coils.* Eur J Clin Exp Med. 2020;18(1):24–27. doi: 10.15584/ejcem.2020.1.5

Maxwell's equations form the basis for any electromagnetic field analysis. They describe them in an exhaustive way and allow for full analysis. The Lorenzt gauge condition is used to eliminate the scalar potential and with harmonic time dependence.[16-18] B_x component is symmetric along the XZ, YZ, and XY planes therefore static B_1 field characteristic, static coil geometry and vector current density is defined.

$$B_0 = B_0\hat{z}, i.e. B_{1x}, B_{1y} \quad \text{(Equ. 2).}$$

The goal is to find the appropriate current density distribution which will generate a static field component along the X, Y and Z directions with the specified uniformity. In order to generate B_x component of the RF field, the current density distribution is viewed as a vector superposition of two components, along the z-direction and the other along the azimuthal direction.[19-27] Thus, the general expression of the current density distribution is:

$$\vec{J}^a(\vec{r}) = \left[j_{\emptyset}^a(\emptyset, z)\hat{\alpha}_{\emptyset} + j_z^a(\emptyset, z)\hat{\alpha}_z\right]\delta(\rho - a) \text{ (Equ. 3).}$$

The expression for both components of the current densities can be written as:

$$j_{\varphi}^a(\varphi, z) = \cos\varphi \sum_{n=1}^{\infty} c_n \sin k_n z \quad \text{(Equ. 2.4),}$$

$$\text{where } |z| \leq \frac{L}{2} \quad \text{(Equ. 2.5);}$$

Where C_n is the Fourier coefficient and kn is factor given as

$$k_n = \frac{(2n-1)\pi}{L} \quad \text{(Equ. 2.6).}$$

The RF field can be expressed in terms of radial B_ρ and azimutal B_φ components of the magnetic field:

$$B_x = B_\rho \cos\phi - B_\varphi \sin\varphi \quad \text{(Equ. 2.7).}$$

Receiving coils needed to be designed and positioned so that they are maximally sensitive to emitted radio frequency signals, that is so that they have the largest possible voltage induced in them by the radio frequency signals emitted by the tissue.[28]

The approximation is made as accurate as necessary by increasing the number of such monopoles. Any two consecutive monopoles are defined as a V-shaped dipole over which a testing function is defined. Satisfying the boundary conduction that the current vanishes at both ends of the dipole. The n-th testing function is non zero only when the V-shaped dipole corresponds to the V-shaped dipole and zero otherwise. The analysis of electromagnetic fields in today's era is carried out by specialized software packages (Fig. 1).[29-32] The enormous development of numerical methods, which has become possible as a result of the continuous increase in computing power of computers caused that very complex 3D objects are analyzed. The project starts with making assumptions and developing a drawing of a 3D object. Next, each component is assigned material properties and an analysis area is assumed after which the results are most often presented in the form of colored graphs or maps of the distribution of the analyzed parameters.[33-38]

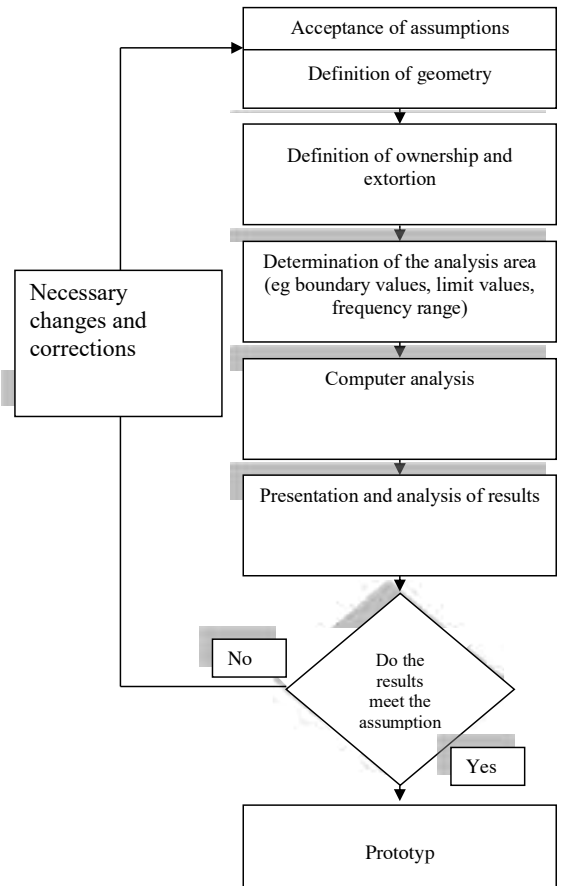

Fig. 1. Simplified computer design scheme

Figure 2 presents two types of birdcage coils. Both types of coils can be used in magnetic resonance systems. The proper selection of geometric dimensions as well as the values of capacities included in the circuit define the characteristics of the coils. From the point of view of the principles of operation of magnetic resonance systems, the receiving coils are resonant circuits with strictly defined properties. The fundamental

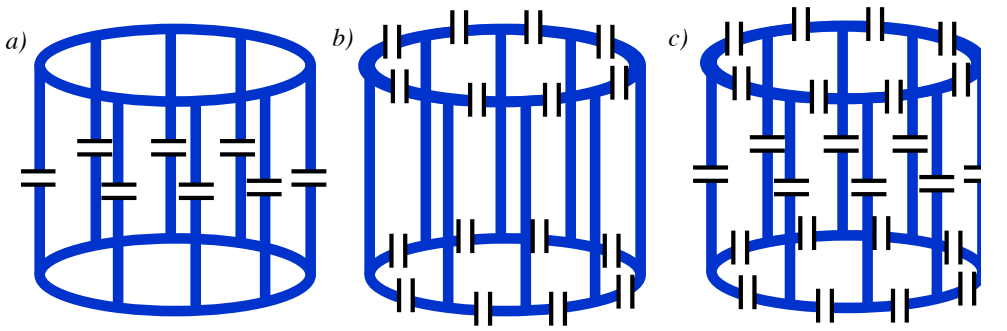

Fig. 2. Birdcage coils, a) high-pass coil, b) low-pass coil, c) quadrature transmit coil

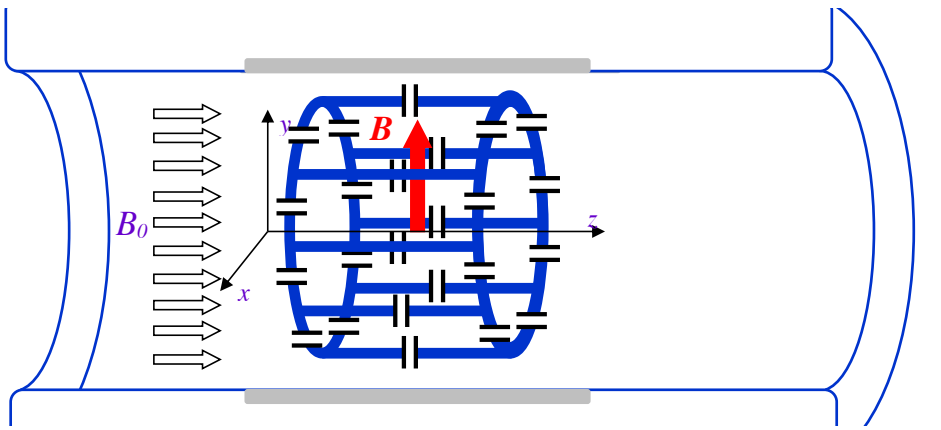

Fig. 3. Schematic diagram of magnetic resonance magnet

and most important is the resonant frequency f0 which strongly depends on the geometry of the circuit. Another important parameter is the Q quality of the resonant system as well as the wave impedance. Birdcage type coils are practically the most used transceiver devices currently in MR systems. Their structure is based on two rings connected with conductive rods. The number of these parallel element's ranges from 8 to 32. Condensers are placed between the conductive elements.

Figure 3 presents an illustrative schematic of the MR system. The main element is a magnet that generates a constant magnetic field and induction B0 = 1.5 [T]. Inside it there are additional coils to generate magnetic gradients and coils to level the field. Noteworthy is the BODY coil, which is the most often transceiver-receiving device and is built into the MR system permanently. The birdcage coil presented can be both a transmitting and receiving element. This type of coil allows the reception of a signal generated by a variable magnetic component in the X-Y plane. In the drawing, this vector is marked in red.

Conclusions

We discussed the major orations of MRI coils and discussed the major physical phenomenon involved in MRI together with RF coil design.

Acknowledgements

Dorota Bartusik-Aebisher acknowledges support from the National Center of Science NCN (New drug delivery systems-MRI study, Grant OPUS-13 number 2017/25/B/ST4/02481).

The list of abbreviations:

a – radious of RF coil, **L** – total length of the coil, **r** (Φ, z) – current vector

References

1. Hayes CE, Axel L. Noise performance of surface coils for magnetic resonance imaging at 1.5 T. *Med Phys*. 1985;12(5):604-607.
2. Boskamp EB. Improved surface coil imaging in MR: decoupling of the excitation and receiver coils. *Radiology*. 1985;157(2):449-452.
3. Axel L, Hayes C. Surface coil magnetic resonance imaging. *Arch Int Physiol Biochim*. 1985;93(5):11-18.
4. Torizuka K, Nishimura K, Asato R, et al. Recent advance in diagnostic imaging: NMR. *No To Shinkei*. 1985;37(5):423-431.
5. Edelstein WA, Schenck JF, Hart HR, Hardy CJ, Foster TH, Bottomley PA. Surface coil magnetic resonance imaging. *JAMA*. 1985;253(6):828.

6. Pope JM, Eberl S. On surface coils and depth pulses. *Magn Reson Imaging.* 1985;3(4):389-398.
7. Axel L. Surface coil magnetic resonance imaging. *J Comput Assist Tomogr*. 1984;8(3):381-384.
8. Hosten N, Lemke AJ. A special surface coil for high-resolution ocular MRI. *Front Radiat Ther Oncol.* 1997;30:20-25.
9. Murakami JW, Hayes CE, Weinberger E. Intensity correction of phased-array surface coil images. *Magn Reson Med.* 1996;35(4):585-590.
10. Prock T, Collins DJ, Leach MO. Numerical evaluation of shaped surface coil sensitivity at 63 MHz. *Phys Med Biol*. 2001;46(7):1753-1765.
11. Liu H, Truwit CL. True energy-minimal and finite-size biplanar gradient coil design for MRI. *IEEE Trans Med Imaging*. 1998;17(5):826-830.
12. Borthakur A, Charagundla SR, Wheaton A, Reddy R. T1rho-weighted MRI using a surface coil to transmit spin--lock pulses. *J Magn Reson*. 2004;167(2):306-316.
13. Yoshioka H, Ueno T, Tanaka T, et al. High-resolution MR imaging of the elbow using a microscopy surface coil and a clinical 1.5 T MR machine: preliminary results. *Skeletal Radiol.* 2004;33(5):265-271.
14. Pinkernelle J, Teichgräber U, Neumann F, et al. Imaging of single human carcinoma cells in vitro using a clinical whole-body magnetic resonance scanner at 3.0 T. *Magn Reson Med.* 2005;53(5):1187-1192.
15. Takagi Y, Sumi M, Van Cauteren M, Nakamura T. Fast and high-resolution MR sialography using a small surface coil. *J Magn Reson Imaging.* 2005;22(1):29-37.
16. Buchli R, Saner M, Meier D, Boskamp EB, Boesiger P. Increased rf power absorption in MR imaging due to rf coupling between body coil and surface coil. *Magn Reson Med.* 1989;9(1):105-112.
17. Garwood M, Uğurbil K, Rath AR, et al. Magnetic resonance imaging with adiabatic pulses using a single surface coil for RF transmission and signal detection. *Magn Reson Med.* 1989;9(1):25-34.
18. Curto CA, Placidi G, Sotgiu A, Alecci M. An open volume, high isolation, radio frequency surface coil system for pulsed magnetic resonance. *J Magn Reson.* 2004;171(2):353-358.
19. Claasen-Vujcić T, Borsboom HM, Gaykema HJ, Mehlkopf T. Transverse low-field RF coils in MRI. *Magn Reson Med.* 1996;36(1):111-116.
20. Li S, Yang QX, Smith MB. RF coil optimization: evaluation of B1 field homogeneity using field histograms and finite element calculations. *Magn Reson Imaging.* 1994;12(7):1079-1087.
21. Buikman D, Helzel T, Röschmann P. The rf coil as a sensitive motion detector for magnetic resonance imaging. *Magn Reson Imaging.* 1988;6(3):281-289.
22. Joseph PM, Fishman JE. Design and evaluation of a radio frequency coil for nuclear magnetic resonance imaging of fluorine and protons. *Med Phys.* 1985;12(6):679-683.
23. Alfonsetti M, Clementi V, Iotti S, et al. Versatile coil design and positioning of transverse-field RF surface coils for clinical 1.5-T MRI applications. *MAGMA*. 2005;18(2):69-75.
24. Anastasiou A, Hall LD. A novel RF coil configuration for in-vivo and ex-vivo imaging of arthritic rabbit knee joints. *Magn Reson Imaging.* 2003;21(1):61-68.
25. Chen G, Muftuler LT, Ha SH, Nalcioglu O. An optimization method for designing SENSE imaging RF coil arrays. *J Magn Reson.* 2007;186(2):273-281.
26. Xu B, Crozier S, Li BK, Wei Q, Liu F. An inverse methodology for high frequency RF head coil design with preemphasized B/sub 1/ field in MRI. *Conf Proc IEEE Eng Med Biol Soc.* 2004;2:1128-1131.
27. Keong Li B, Xu B, Tat Hui H, Crozier S. A new approach for magnetic resonance RF head coil design. *Conf Proc IEEE Eng Med Biol Soc.* 2005;5:5100-5103.
28. Muftuler LT, Chen G, Nalcioglu O. An inverse method to design RF coil arrays optimized for SENSE imaging. *Phys Med Biol.* 2006;51(24):6457-6469.
29. Alecci M, Romanzetti S, Kaffanke J, Celik A, Wegener HP, Shah NJ. Practical design of a 4 Tesla double-tuned RF surface coil for interleaved 1H and 23Na MRI of rat brain. *J Magn Reson.* 2006;181(2):203-211.
30. Xu B, Wei Q, Liu F, Crozier S. An inverse methodology for high-frequency RF coil design for MRI with de-emphasized B1 fields. *IEEE Trans Biomed Eng.* 2005;52(9):1582-1587.
31. Lee HS, Woo DC, Min KH, Kim YK, Lee HK, Choe BY. Development of a solenoid RF coil for animal imaging in 3 T high-magnetic-field MRI. *Scanning.* 2008;30(5):419-425.
32. Hadley JR, Roberts JA, Goodrich KC, Buswell HR, Parker DL. Relative RF coil performance in carotid imaging. *Magn Reson Imaging.* 2005;23(5):629-639.
33. Ibrahim TS, Mitchell C, Schmalbrock P, Lee R, Chakeres DW. Electromagnetic perspective on the operation of RF coils at 1.5-11.7 Tesla. *Magn Reson Med.* 2005;54(3):683-690.
34. Brown R, Mareyam A, Reid E, Wang Y. Novel RF coil geometry for lower extremity imaging. *Magn Reson Med.* 2004;51(3):635-639.
35. Tincher M, Meyer CR, Gupta R, Williams DM. Polynomial modeling and reduction of RF body coil spatial inhomogeneity in MRI. *IEEE Trans Med Imaging.* 1993;12(2):361-365.
36. Harman RR, Butson PC, Hall AS, Young IR, Bydder GM. Some observations of the design of rf coils for human internal use. *Magn Reson Med.* 1988;6(1):49-62.
37. Harpen MD. Analysis of capacitive coupling and associated loss for a solenoidal magnetic resonance imaging radio-frequency coil. *Med Phys.* 1989;16(2):234-238.
38. Nakajima M, Nakajima I, Obayashi S, Nagai Y, Obata T, Hirano Y, Ikehira H. Development of a patch antenna array RF coil for ultra-high field MRI. *Magn Reson Med Sci*. 2007;6(4):231-233.